One-phonon resonant Raman scattering: Fröhlich exciton-phonon interaction

C. Trallero-Giner,* A. Cantarero,† and M. Cardona
Max-Planck-Institut für Festkörperforschung, Heisenbergstrasse 1 Postfach 80 06 65, D-7000 Stuttgart 80, Federal Republic of Germany
(Received 1 March 1989)

An explicit expression for forbidden Raman scattering by one LO phonon with excitons as intermediate states is given. The theory can be applied at photon frequencies below and above the exciton energy. The matrix elements corresponding to transitions between different exciton states are calculated analytically. The different contributions to the squared Raman polarizability are compared; the most important one is found to be due to discrete-continuous transitions. It is shown in this case that the outgoing resonance in the Raman efficiency is always higher than the incoming one, a peculiarity seen experimentally in all III-V compound semiconductors. From the theoretical model a general criterion for the application of the free–electron-hole–pair theory is given in terms of the exciton Bohr radius. An analysis of the interference effect between the allowed and forbidden scattering is presented, and qualitative and quantitative differences with the free–electron-hole–pair theory are discussed. Absolute values of Raman polarizabilities are calculated and compared with recent measurements for GaP, yielding a good agreement without the use of any fit parameter.

I. INTRODUCTION

Excitons contribute strongly to the resonant enhancement of Raman scattering efficiencies in many III-V compounds when the interaction with phonons is via the deformation potential[1] (DP). Taking as intermediate states interband transitions modified by excitonic electron-hole correlation suffices to reproduce the absolute values of the Raman polarizability of some III-V compounds measured in allowed scattering configurations.[1]

It is well known in polar semiconductors that electrons can also interact with LO phonons via the Fröhlich (F) mechanism[2] leading to forbidden scattering. In this case the Raman tensor is diagonal[3] and the forbidden scattering can be observed in the backscattering configuration $\bar{z}(xx)z$ for a (001) surface ($\mathbf{x}\|[100]$, $\mathbf{y}\|[010]$, $\mathbf{z}\|[001]$ directions) in the zinc-blende-type semiconductors. This Raman process is called forbidden because in the dipole approximation the contribution of electrons and holes cancel exactly when the wave vector of the phonon is taken to be zero. The finiteness of the photon wave vector and the wave vector conservation law make the process "allowed" in backscattering.

Such forbidden scattering was first observed in CdS.[4,5] Since then, it has been reported in a number of semiconductor materials.[3,6] In the past several papers have appeared on the subject of III-V compound semiconductors,[7–13] semiconductor alloys,[14,15] and semiconductor superlattices.[16] In these works absolute values of Raman scattering efficiencies were obtained in several backscattering configurations. In particular, F-induced scattering was measured at the E_0 and/or $E_0+\Delta_0$ critical points (CP's) and absolute values of the Raman polarizability $|a_F|^2$ were obtained.[7–13]

In the specific case of bulk materials, some important conclusions can be derived from Refs. 7–13. The theory of forbidden Raman scattering, taking into account free electron-hole pairs, explains neither the large scattering efficiencies nor the observed resonance profiles at the E_0 CP. The enhancement is due to excitonic effects. Qualitative agreement has been obtained in Ref. 10 by rescaling the calculations of Martin[17] in the region below the $1s$ exciton. At the $E_0+\Delta_0$ CP, however, the experimental profiles of GaAs,[10] GaSb,[13] and InP (Ref. 9) were reproduced by adding a higher-order process consisting of elastic scattering by impurities[18] followed by Fröhlich scattering. A theory of the Raman tensor for F interaction covering incoming and outgoing resonances with CP's in the whole spectral range is thus needed in order to interpret the experimental results.

Ganguly and Birman[19] obtained a formal expression of a_F, further developed by Martin[17] in a Green-function formalism, including only the discrete exciton spectrum. Martin also gave an explicit expression for uncorrelated electron-hole pairs as intermediate states. Zeyher *et al.*[20] calculated the Raman tensor only for incident frequencies very near a discrete exciton or in the free–electron-hole–pair continuum. Up to now an explicit expression that allows us to calculate $|a_F|^2$ in a broad range covering discrete and continuous excitons has not been reported. We present here a general expression valid in a broad spectral range around a CP, obtained taking Wannier-Mott excitons as intermediate states. This theory will be developed in Sec. II and a criterion to ascertain when excitonic effects are important will be analyzed. Section III will be devoted to the interference between F and DP scattering. In Sec. IV the predictions of the theory will be compared with experimental data for GaP and in Sec. V the main conclusions of the work will be given.

II. RAMAN POLARIZABILITY

The Raman polarizability a is given by[1]

$$a=\frac{n_l n_s}{2\pi}\frac{V_c}{\bar{u}_0}\frac{1}{\hbar\omega_0}W_{fi}(\omega_s,\mathbf{e}_s,\omega_l,\mathbf{e}_l)\ , \tag{1}$$

where $n_{l\,(s)}$, $\omega_{l\,(s)}$, and $\mathbf{e}_{l\,(s)}$ are the refractive index, frequency, and polarization vector of the laser (scattered) electric field, respectively, V_c is the volume of the primitive cell, $\bar{u}_0$ the relative displacement defined as

$$\bar{u}_0=\left[\frac{\hbar V_c}{2VM^*\omega_0}\right]^{1/2}, \tag{2}$$

ω_0 the phonon frequency, V the volume of the crystal, and M^* the reduced mass of the atoms contributing to the optical mode. For a one-phonon process the amplitude probability can be written as

$$W_{fi}=\sum_{p,q}\left[\frac{\langle f|H_{ER}|q\rangle\langle q|H_{EL}|p\rangle\langle p|H_{ER}|i\rangle}{(\hbar\omega_l-E_p+i\Gamma_p)(\hbar\omega_s-E_q+i\Gamma_q)}+\frac{\langle f|H_{ER}|p\rangle\langle p|H_{EL}|q\rangle\langle q|H_{ER}|i\rangle}{(\hbar\omega_l+E_q+i\Gamma_q)(\hbar\omega_s+E_p+i\Gamma_p)}\right]. \tag{3}$$

The subindices p and q refer to the excitonic intermediate states, E_α and Γ_α ($\alpha=p,q$) and their respective energies and lifetime broadenings, and H_{ER} and H_{EL} the exciton-radiation and exciton-lattice interaction Hamiltonians, which can be expressed as[19]

$$H_{ER}=\sum_{\substack{\mathbf{K},p,\\ \mathbf{e},\kappa,\\ c,v}}[T^p_{cv}(\mathbf{K})D^\dagger_{p\mathbf{K}}(a_{\kappa,\mathbf{e}}+a^\dagger_{-\kappa,\mathbf{e}})+\text{c.c.}], \tag{4}$$

$$H_{EL}=\sum_{\substack{\mathbf{Q},\nu,\\ \mathbf{K},\mathbf{K}',\\ p,q}} S^{\mathbf{K}',\mathbf{K}}_{q,p}(\mathbf{Q})D^\dagger_{q\mathbf{K}'}D_{p\mathbf{K}}(b^\dagger_{\mathbf{Q},\nu}+b_{-\mathbf{Q},\nu}), \tag{5}$$

where $D_{p\mathbf{K}}$ ($D^\dagger_{p\mathbf{K}}$), $a_{\kappa,\mathbf{e}}$ ($a^\dagger_{-\kappa,\mathbf{e}}$), and $b_{-\mathbf{Q},\nu}$ ($b^\dagger_{\mathbf{Q},\nu}$) are annihilation (creation) operators for excitons, photons, and phonons, respectively, κ is the wave vector of the light, $\mathbf{Q}$ the wave vector of the phonon, ν the phonon branch, and $\mathbf{K}$ the center-of-mass momentum of the exciton. The exciton-photon coupling constant T is given by[21]

$$T^p_{cv}(\mathbf{K})=-\frac{e}{m}\left[\frac{2\pi\hbar}{\omega_{l\,(s)}n^2_{l\,(s)}}\right]^{1/2}\mathbf{e}_{l\,(s)}\langle c|\mathbf{p}|v\rangle\Psi_p(\mathbf{0})\delta_{\mathbf{K},\kappa}, \tag{6}$$

$\langle c|\mathbf{p}|v\rangle$ being the matrix element of the momentum operator and $\Psi_p(\mathbf{r})$ the wave function of the internal exciton state. The exciton-phonon coupling constant for the Fröhlich exciton-lattice interaction with long-wavelength longitudinal-optical phonons is[2]

$$S^{\mathbf{K}',\mathbf{K}}_{q,p}(\mathbf{Q})=\frac{1}{\sqrt{V}}\frac{C^*_F}{|\mathbf{Q}|}[I_{q,p}(-\mathbf{Q}_h)-I_{q,p}(\mathbf{Q}_e)]\delta_{\mathbf{K}',\mathbf{K}-\mathbf{q}}, \tag{7}$$

$$C_F=-i(\epsilon_\infty^{-1}-\epsilon_0^{-1})^{1/2}(2\pi\hbar\omega_0e^2)^{1/2}, \tag{8}$$

ϵ_0 being the static and ϵ_∞ the optical dielectric constant. $I_{q,p}(\mathbf{Q}_\alpha)$ ($\alpha=e,h$) is equal to

$$I_{q,p}(\mathbf{Q}_\alpha)=\int d^3\mathbf{r}\,\Psi^*_q(\mathbf{r})e^{i\mathbf{Q}_\alpha\cdot\mathbf{r}/a}\Psi_p(\mathbf{r}), \tag{9}$$

$\mathbf{Q}_\alpha=(m_\alpha/m_T)\mathbf{Q}a$, $m_T=m_e+m_h$, $m_e(m_h)$ is the electron (hole) effective mass, and a the exciton Bohr radius. Introducing expressions (3)–(9) into Eq. (1) and considering the term which dominates near resonance, the contribution to the Raman polarizability can be written as

$$a_F=\left[\frac{e}{m}\right]^2\frac{V_cC^*_F\langle c|\mathbf{e}_l\cdot\mathbf{p}|v\rangle\langle v|\mathbf{e}_s\cdot\mathbf{p}|c\rangle}{\bar{u}_0\omega_l(\omega_l\omega_s)^{1/2}Q}\sum_{p,q}\Psi^*_q(\mathbf{0})\frac{[I_{q,p}(-\mathbf{Q}_h)-I_{q,p}(\mathbf{Q}_e)]}{(\hbar\omega_s-E_q+i\Gamma_q)(\hbar\omega_l-E_p+i\Gamma_p)}\Psi_p(\mathbf{0}). \tag{10}$$

In order to evaluate Eq. (10) it is necessary to know the matrix element $I_{p,q}(\mathbf{Q})$ between different exciton states (discrete-discrete, discrete-continuous, and continuous-continuous). In the following we consider, in the framework of the envelope-function approximation, the hydrogenic model.

A. Matrix elements

For angular momentum $l=0$, the discrete exciton wave function is taken to be[22]

$$\Psi_m(\rho)=\frac{1}{(\pi a^3m^3)^{1/2}}e^{-\rho/m}F(1-m,2,2\rho/m) \tag{11}$$

with $E_m=E_g-R/m^2$, $F(a,b,z)$ being the confluent hypergeometric function, $\rho=\mathbf{r}/a$, E_g the energy gap, and R the exciton Rydberg energy. The matrix elements corresponding to a discrete-discrete transition can be written as

$$I_{n,m}(Q_\alpha)=\frac{4}{Q_\alpha(n^3m^3)^{1/2}}\text{Im}[A(Q_\alpha)], \tag{12}$$

where

$$A=\int_0^\infty e^{-\lambda z}z^{\gamma-1}F(\alpha,\gamma,k_0z)F(\alpha',\gamma,k'_0z)dz \tag{13}$$

with $\gamma=2$, $\alpha=-n+1$, $\alpha'=-m+1$, $k_0=2/n$, $k'_0=2/m$, and $\lambda=1/m+1/n-iQ_\alpha$.

The evaluation of Eq. (13) yields[23]

$$A=\Gamma(\gamma)\lambda^{\alpha+\alpha'-\gamma}(\lambda-k_0)^{-\alpha}(\lambda-k'_0)^{-\alpha'}\times F(\alpha,\alpha',\gamma,k_0k'_0/(\lambda-k_0)(\lambda-k'_0)), \tag{14}$$

where $\Gamma(z)$ is the gamma function and $F(a,b,c,z)$ the hypergeometric function.

From Eq. (14) it follows that

$$I_{n,m}(Q_\alpha)=\frac{-4}{Q_\alpha}\frac{(mn)^{1/2}}{[(m-n)^2+n^2m^2Q_\alpha^2]}F(1-m,1-n,2,-4mn/[(m-n)^2+n^2m^2Q_\alpha^2])$$
$$\times\mathrm{Im}\left[\left[\frac{m-n-inmQ_\alpha}{m+n-imnQ_\alpha}\right]^m\left[\frac{n-m-iQ_\alpha mn}{n+m-iQ_\alpha mn}\right]^n\right]. \quad (15)$$

For the continuous states we have[22]

$$\Psi_k(\rho)=\frac{1}{(\pi V)^{1/2}}ke^{\pi/2k}|\Gamma(1-i/k)|e^{-ik\rho}F(1+i/k,2,2ik\rho) \quad (16)$$

with $E_k=E_g+Rk^2$. The discrete-continuous matrix elements can also be solved using Eq. (14) with $\alpha'=1+i/k$, $k_0'=2ik$, and $\lambda=1/n+i(k-Q_\alpha)$, obtaining

$$I_{nk}(Q_\alpha)=\left[\frac{a^3}{n^3V}\right]^{1/2}\frac{4ke^{\pi/2k}|\Gamma(1-i/k)|}{Q_\alpha}(-1)^{n-1}n^2$$
$$\times\mathrm{Im}\left[\frac{F(1-n,1+i/k,2,z)}{[1-in(k-Q_\alpha)][1-in(k+Q_\alpha)]}\frac{[1-in(k-Q_\alpha)]^{2n}}{[1+n^2(k-Q_\alpha)^2]^n}\left[\frac{1+in(k-Q_\alpha)}{1-in(k+Q_\alpha)}\right]^{i/k}\right]. \quad (17)$$

For simplicity we replace in the continuous-continuous case the exciton wave function by the wave function of free electron-hole pairs,

$$\Psi_{\mathbf{k}}(\rho)=\frac{e^{i\mathbf{k}\cdot\rho}}{\sqrt{V}}, \quad (18)$$

which gives

$$I_{\mathbf{k},\mathbf{k}'}(\mathbf{Q}_\alpha)=(2\pi)^3\frac{a^3}{V}\delta(\mathbf{k}'-\mathbf{k}+\mathbf{Q}_\alpha). \quad (19)$$

It will be shown later that this contribution is negligible compared with the other two.

B. Raman tensor

The diagonal components of the Raman tensor a_F can be obtained by introducing the calculated matrix elements into Eq. (10); then

$$a_F=K_F\left[\sum_{n,m}\frac{D_{n,m}}{(\eta+1/n^2+i\gamma_n)(\eta-\eta_0+1/m^2+i\gamma_m)}\right.$$
$$+\sum_n\int_0^\infty dk\frac{D_{n,k}}{1-e^{-2\pi/k}}\frac{1}{n^3}\left[\frac{1}{[\eta-k^2+i\gamma(k)](\eta-\eta_0+1/n^2+i\gamma_n)}+\frac{1}{(\eta+1/n^2+i\gamma_n)[\eta-\eta_0-k^2+i\gamma(k)]}\right]$$
$$+\frac{i}{8(Q_e^2-Q_h^2)}\left[\frac{1}{Q_e}\ln\frac{\sqrt{\eta+i\gamma(k)}+[\eta-\eta_0+i\gamma(k)]^{1/2}-Q_e}{\sqrt{\eta+i\gamma(k)}+[\eta-\eta_0+i\gamma(k)]^{1/2}+Q_e}\right.$$
$$\left.\left.-\frac{1}{Q_h}\ln\frac{\sqrt{\eta+i\gamma(k)}+[\eta-\eta_0+i\gamma(k)]^{1/2}-Q_h}{\sqrt{\eta+i\gamma(k)}+[\eta-\eta_0+i\gamma(k)]^{1/2}+Q_h}\right]\right], \quad (20)$$

where

$$\eta=(\hbar\omega_l-E_g)/R,\ \eta_0=\hbar\omega_0/R,\ \gamma=\Gamma/R, \quad (21)$$

$$D_{n,m}=\frac{1}{(n^3m^3)^{1/2}}\frac{I_{n,m}(-Q_h)-I_{n,m}(Q_e)}{Q_e^2-Q_h^2}, \quad (22)$$

$$D_{n,k}=\left[\frac{Vn^3}{a^3}\right]^{1/2}\frac{e^{-\pi/2k}}{|\Gamma(1-i/k)|}\frac{[I_{n,k}(-Q_h)-I_{n,k}(Q_e)]}{Q_e^2-Q_h^2}, \quad (23)$$

$$K_F=\frac{2}{\pi}\left[a_0^3\frac{M^*}{m}\frac{\hbar\omega_0}{R_{\mathrm{H}}}\right]^{1/2}\frac{Qa_{\mathrm{H}}}{\hbar\omega_l(\hbar\omega_l\hbar\omega_s)^{1/2}}\frac{2}{3}\frac{|P^2|}{m}\frac{a_{\mathrm{H}}}{a}\left[\frac{R_{\mathrm{H}}}{R}\right]^2C_F^*\frac{m_e-m_h}{m_T}, \quad (24)$$

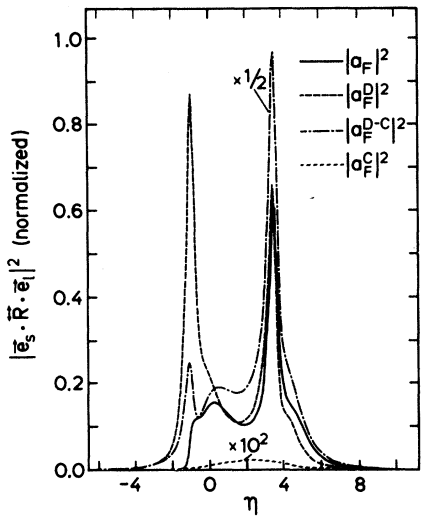

FIG. 1. Raman polarizability $|a_F|^2$, as a function of the parameter $\eta=(\hbar\omega_l-E_g)/R$ for $\hbar\omega_0/R=4.55$. Also the different contributions—discrete-discrete, $|a_F^D|^2$; discrete-continuous plus continuous-discrete, $|a_F^{D\text{-}C}|^2$; and continuous-continuous, $|a_F^C|$—are shown in the figure. The $|a_F^{D\text{-}C}|^2$ curve has been multiplied by a factor of $\frac{1}{2}$ and $|a_F^C|^2$ by 10^2.

a_H and R_H being the hydrogen Bohr radius and Rydberg, respectively, $P=\langle s|P_x|x\rangle$, and a_0 the lattice constant. The first term inside the second set of large parentheses in Eq. (20) represents the contribution of the discrete exciton states, the second and the third terms correspond to continuous-discrete and discrete-continuous transitions, and the last one is due to the (uncorrelated) continuous states whose evaluation is given in the Appendix.

Figure 1 shows the normalized $|a_F|^2$ Raman polarizability as a function of the reduced laser photon energy η for the case $\hbar\omega_0/R=4.55$. The following empirical relation is used for the lifetime broadenings, $\gamma_n=\gamma(k)-[\gamma(k)-\gamma_1]/n^2$, with $\gamma(k)=1$ and $\gamma_1=0.54$. The squared magnitudes of the different contributions—discrete-discrete, $|a_F^D|^2$; discrete-continuous plus continuous-discrete, $|a_F^{D\text{-}C}|^2$; and continuous-continuous, $|a_F^C|^2$—are also shown. $|a_F^{D\text{-}C}|^2$ has been multiplied by a factor of $\frac{1}{2}$ and the $|a_F^C|^2$ by a factor of 10^2. As can be seen in Fig. 1, the $|a_F^C|^2$ is several orders of magnitude lower than the others. The most important contributions to the Raman tensor comes from the discrete-continuous plus continuous-discrete excitonic states. However, this is only true when the phonon wave vector has a small value, in our case $\kappa_l+\kappa_s$. The $|a_F^{D\text{-}C}|^2$ presents an outgoing resonance stronger than the incoming one. This is due to the fact that the second term inside the second set of large parentheses in Eq. (20) is doubly resonant for laser frequencies near $E_g+\hbar\omega_0-R$. Both $|a_F^D|^2$ and $|a_F^{D\text{-}C}|^2$ show well-defined peaks in $\eta_1=-1$ and $\eta_2=\hbar\omega_0/R-1$. Nevertheless, the sum $a_F^D+a_F^{D\text{-}C}$ interferes destructively, and a pronounced slope in the square polarizability for $\eta\approx\eta_1$ is produced. However, the outgoing resonance remains well defined. The behavior of $|a_F|^2$ in the region $0<\eta<0.5$ is due to the transitions among $n=2,3,\ldots$. These peculiarities of the exciton states interacting with the long-wavelength longitudinal-optical phonon explain the experimental observations for many III-V compound semiconductors that cannot be explained within the uncorrelated electron-hole model.[9,10,12] The latter can be recovered from Eq. (20) by making the exciton Bohr radius $a\to\infty$. The corresponding expression for the Raman tensor retaining only terms proportional to Q^2 is, in agreement with Ref. 17,

$$a_F^C=K_F^C\left[\left[\frac{\hbar\omega_l-E_g+i\Gamma}{\hbar\omega_0}\right]^{1/2}-\left[\frac{\hbar\omega_s-E_g+i\Gamma}{\hbar\omega_0}\right]^{1/2}\right]^3 \tag{25}$$

with

$$K_F^C=\frac{Q}{12}\left[\frac{e}{m\hbar}\right]^2\frac{|C_F|}{\hbar\omega_0}\frac{1}{\omega_l(\omega_l\omega_s)^{1/2}}(a_0^3\mu M^*)^{1/2}\times\tfrac{2}{3}|p^2|\left[\frac{m_e-m_h}{m_T}\right]. \tag{26}$$

It is important to analyze the range of application of the uncorrelated pair theory. This analysis can be done in terms of the Bohr radius a, a parameter easily evaluable from the knowledge of the exciton Rydberg or the effective masses corresponding to the different CP's. Figure 2 shows the Raman tensor in units of K_F^C as a function of $(\hbar\omega_l-E_g)/\hbar\omega_0$. This plot is practically universal. The only *ad hoc* parameter is the ratio between the pho-

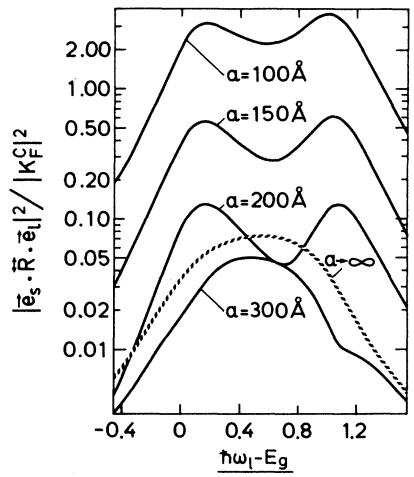

FIG. 2. Raman polarizability $|a_F|^2$ given by Eq. (20) in units of K_F^C, as a function of $(\hbar\omega_l-E_g)/\hbar\omega_0$, for different exciton Bohr radii. The $a\to\infty$ curve corresponds to uncorrelated electron-hole pairs, Eq. (25). For the calculation a value of $\Gamma/\hbar\omega_0=\frac{1}{5}$ was taken. The nonmonotonic behavior for $a=200$ and 300 Å, and ∞ seems to be an artifact of having used uncorrelated states for the continuous-continuous contribution in Eq. (20).

non energy and the exciton Rydberg, which only accounts for the separation between peaks, not for their strength.

In Fig. 2 the different curves correspond to Bohr radii equal 100, 150, 200, and 300 Å, and the limit $a \to \infty$. From the result it is possible to conclude that, in general, a Bohr radius of 200–250 Å is large enough to neglect Coulomb interaction in order to reproduce absolute values, although the profile will still depend on the lifetime.

III. INTERFERENCE EFFECTS

It has been shown that allowed and forbidden scattering can interfere[7–14] for experiments performed on the (001) surface due to the form of the total Raman tensor:

$$\vec{\vec{R}} = \begin{bmatrix} a_F & a_{DP} & 0 \\ a_{DP} & a_F & 0 \\ 0 & 0 & a_F \end{bmatrix}, \tag{27}$$

a_{DP} being the Raman polarizability for deformation-potential interaction. In the $\bar{z}(x'x')z$ and $\bar{z}(y'y')z$ backscattering configurations ($\mathbf{x}' \| [110]$, $\mathbf{y}' \| [\bar{1}10]$) both $a_F \pm a_{DP}$ can be selected. For a three-band model, and assuming the same Bohr radius for the excitons formed from the conduction and valence bands (heavy-hole, light-hole, and split-off), a_{DP} is given by[1]

$$a_{DP} = \sum_{p,q} K_{qp} \left\{ \sum_{n=1}^{\infty} \frac{1}{n^3} \frac{1}{(\eta_p + 1/n^2 + i\gamma_n)(\eta_q - \eta_0 + 1/n^2 + i\gamma_n)} - \frac{1}{2} \sum_{n=1}^{\infty} \frac{1}{n^3} \frac{1}{[\eta_p + 1/n^2 + i\gamma(k)][\eta_q - n_0 + 1/n^2 + i\gamma(k)]} + \frac{1}{4} \frac{1}{\eta_p - \eta_q + \eta_0} \left[\ln \frac{\eta_q - \eta_0 + i\gamma(k)}{\eta_p + i\gamma(k)} + \pi i \left[\coth \frac{\pi}{[\eta_p + i\gamma(k)]^{1/2}} - \coth \frac{\pi}{[\eta_q - \eta_0 + i\gamma(k)]^{1/2}} \right] \right] \right\} \tag{28}$$

where

$$\eta_p = (\hbar\omega_l - E_{gp})/R \tag{29}$$

E_{gp} being the corresponding gap. The factor K_{qp} is given in Ref. 1, and the sum in p,q runs over the heavy, light, and split-off excitons. With the two tensors a_{DP} and a_F we can calculate the interference effect according to $|a_F \pm a_{DP}|^2$. In Fig. 3 the real and imaginary parts of the Raman polarizabilities a_{DP} and a_F are shown. In the calculation a background due to other transitions equals zero, and the parameters of the $E_0 + \Delta_0$ gap for GaAs were used. Since $m_e - m_h < 0$ the real part of the Raman polarizability a_F is negative near the incoming but positive near the outgoing resonance. The imaginary part of a_F presents a negative minimum for laser frequency near the outgoing resonance. The imaginary parts of a_{DP} and a_F have opposite signs. If the exciton Bohr radius $a \to \infty$, both components of a_F have the same sign near the maximum of $|a_F|^2$ (Ref. 8), and the same behavior and conclusions as found for the electron-hole uncorrelated theory are obtained. These facts signal a qualitative difference between the excitonic and free-electron-hole-pair models and the way in which Raman polarizabilities a_F and a_{DP} interfere in each case. A detailed study of the interference effects and the role of excitonic states in some III-V compounds will be published elsewhere.[24]

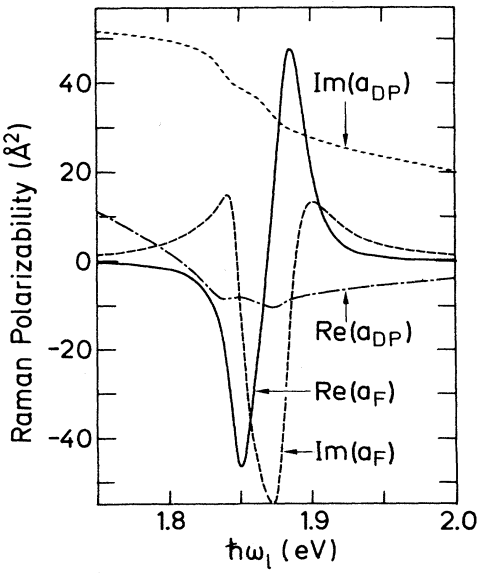

FIG. 3. Energy dependence of the Raman polarizabilities a_{DP} for allowed scattering and a_F for intrinsic forbidden scattering by LO phonons. The parameters used correspond to GaAs in the $E_0 + \Delta_0$ critical point (Ref. 8).

IV. COMPARISON WITH EXPERIMENT

In a previous paper[1] we calculated the Raman polarizability a_{DP} for DP-induced scattering. The calculated $|a_{DP}|^2$ were compared in a large spectral range with the experimental data of GaP (Ref. 12) in absolute value. Data of F-induced scattering are also available in Ref. 12.

In order to calculate a_F it is necessary to consider three intraband terms, corresponding to light (lh), heavy (hh), and split-off (s.o.) excitons, $E_0 + \Delta_0$ being CP's too close to the outgoing resonance with E_0. Thus

$$a_F = a_{hh} + a_{lh} + a_{s.o.} + b \ , \tag{30}$$

where b is a small background coming from nonresonant processes. The calculated $|a_F|^2$ is plotted in Fig. 4 together with the experimental values taken from Ref. 12. The values of the parameters needed for the present cal-

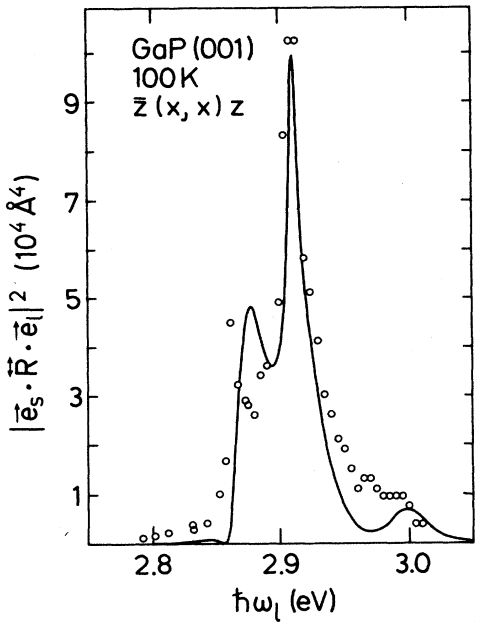

FIG. 4. Comparison with experimental data for GaP (Ref. 12). The circles represent the experimental points while the solid line was calculated with Eq. (20).

culation are given in Table I. The set of parameters used is the same as in Ref. 1, except that here we took the same Bohr radius (50 Å) for the E_0 and for the $E_0+\Delta_0$ CP's. With this Bohr radius the same profile for $|a_{DP}|^2$ is obtained. As discussed in Ref. 1, that is a good approximation in III-V compound semiconductors. Sell and Lawaetz[25] found an exciton Bohr radius of 56 Å for GaP, which agrees well with the 50 Å used by us in the fit for $|a_{DP}|^2$.

The theoretical curve shown in Fig. 4 reproduces well the maximum measured value without any fit. It also reproduces the main characteristic of the resonance profile: the outgoing resonance is about 2 times higher than the incoming one. The peak corresponding to the 1s exciton is, however, absent for the present set of parameters because of the interference between the discrete-discrete and the discrete-continuous excitonic states, as was already stated. The region close to the $E_0+\Delta_0$ is reproduced qualitatively, although the interference between the outgoing resonance at E_0 and the incoming one at $E_0+\Delta_0$ is more pronounced in the calculation.

V. CONCLUSIONS

The Raman polarizability a_F for one-phonon resonance Raman scattering is calculated for Fröhlich interaction considering excitons as intermediate states in the Raman process. The main characteristic of the $|a_F|^2$ profile as a function of the wavelength is that the outgoing peak is higher than the incoming one. This is due to the double-resonance behavior of the outgoing resonance (the phonon connects an exciton in the continuum with an exciton in the discrete spectrum). It is shown that the uncorrelated electron-hole–pair model for the Raman polarizability can be used when the exciton Bohr radius is of the order of 200–250 Å. The interference effects due to deformation-potential and Fröhlich interactions calculated using the correlated or uncorrelated electron-hole–pair models show different qualitative behavior. The calculated $|a_F|^2$ has been compared with the experimental data available for GaP, giving an excellent agreement in absolute value without any fit parameter. The theory should be applicable to other polar semiconductors such as the II-VI compounds.

TABLE I. Numerical values of the parameters used for the theoretical fit of Fig. 4.

Parameters	Values	Reference
R	11 meV	24
E_0	2.873 eV	12
Δ_0	80 meV	26
$\hbar\omega_0$	50 meV	12
a_0	5.45 Å	27
M^*	21.45 amu	28
n	4.0	29[a]
Q	1.19×10^{-2} Å^{-1}	b
ϵ_0	11.11	30
ϵ_∞	9.11	30
$\lvert C_F\rvert$	0.299 eV Å$^{1/2}$	
$\lvert P^2\rvert/m$	10.63 eV	c
Γ_{lh}	5 meV	1
Γ_{hh}	5 meV	1
$\Gamma_{s.o.}$	10 meV	1
a	50 Å	
b	55 Å^2	1
m_e	$0.12m$	12
m_{hh}	$0.45m$	31[d]
m_{lh}	$0.16m$	12
$m_{s.o.}$	$0.24m$	12

[a]Mean value in the region of 2.7–3.1 eV (Ref. 31).
[b]$q=(n/c)(\omega_l+\omega_s)$.
[c]This value was calculated from the $\mathbf{k}\cdot\mathbf{p}$ expression $|P^2|/m=\frac{1}{2}(m/m_e-1)[E_0(E_0+\Delta_0)/(E_0+\frac{2}{3}\Delta_0)]$ for $m_e=0.12m$.
[d]Among the values in the literature, we selected that which gives the best fit to experimental data.

ACKNOWLEDGMENTS

Two of the authors, A.C. and C.T.-G., thank the Ministerio de Educación y Ciencia (Spain) and the Alexander von Humboldt Foundation (Bonn, Germany), respectively, for financial support.

APPENDIX

The term corresponding to the continuous-continuous transition can be written, by using the definitions given by Eqs. (18) and (19), as

$$c=\frac{1}{(2\pi)^3\alpha^3R^2}\times\int d^3\mathbf{k}\times\int d^3\mathbf{k}'\frac{\delta(\mathbf{k}'-\mathbf{k}-\mathbf{Q}_h)-\delta(\mathbf{k}'-\mathbf{k}+\mathbf{Q}_e)}{[\eta+i\gamma(k)-k^2][\eta-\eta_0+i\gamma(k')-k'^2]}\ . \tag{A1}$$

One of the integrals can be performed automatically by making use of the properties of the δ function. Integrating the angular part of the second integral with $\gamma(k)$ constant yields

$$c=\frac{1}{8\pi^2\alpha^3R^2}\left[\frac{1}{Q_h}F(Q_h)-\frac{1}{Q_e}F(Q_e)\right], \tag{A2}$$

where

$$F(x)=\int_0^\infty dk\frac{k}{k^2-\xi^2}\ln\frac{\zeta^2-(k+x)^2}{\zeta^2-(k-x)^2} \tag{A3}$$

with

$$\xi^2=\eta-\eta_0+i\gamma \quad\text{and}\quad \zeta^2=\eta+i\gamma\ . \tag{A4}$$

The integral (A3) can be separated into two integrals by expanding the squared terms in the logarithm. If k is changed by $-k$ in the second one, we obtain

$$F(x)=\int_{-\infty}^{+\infty}dk\frac{k}{k^2-\xi^2}\ln\frac{\zeta+k+x}{\zeta+k-x}\ . \tag{A5}$$

The branch cut in the logarithm is in the lower half-plane. We can avoid its contribution by closing the contour in the upper half-plane. The result is

$$F(x)=\pi i\ln\frac{\zeta+\xi+x}{\zeta+\xi-x}\ . \tag{A6}$$

Inserting the values of ζ and ξ into (A6) and substituting in (A2), the final expression contained in Eq. (20) is obtained.

*On leave from Department of Theoretical Physics, Havana University, Havana, Cuba.
†On leave from Departament de Física Aplicada, Universitat de València, E-46100 València, Spain.

[1]A. Cantarero, C. Trallero-Giner, and M. Cardona, Phys. Rev. B **39**, 8388 (1989).
[2]H. Fröhlich, Adv. Phys. **3**, 325 (1954).
[3]M. Cardona, in *Light Scattering in Solids II,* Vol. 50 of *Topics in Applied Physics,* edited by M. Cardona and G. Güntherodt (Springer, Heidelberg, 1982), p. 19.
[4]R. C. C. Leite and S. P. S. Porto, Phys. Rev. Lett. **17**, 10 (1966).
[5]R. M. Martin and T. C. Damen, Phys. Rev. Lett. **26**, 86 (1971).
[6]W. Richter, in *Solid State Physics,* Vol. 78 of *Springer Tracts in Modern Physics,* edited by G. Höhler (Springer, Heidelberg, 1976), p. 121.
[7]J. Menéndez and M. Cardona, Phys. Rev. Lett. **51**, 1297 (1983).
[8]J. Menéndez and M. Cardona, Phys. Rev. B **31**, 3696 (1985).
[9]W. Kauschke and M. Cardona, Phys. Rev. B **33**, 5473 (1986).
[10]A. K. Sood, W. Kauscchke, J. Menéndez, and M. Cardona, Phys. Rev. B **35**, 2886 (1987).
[11]W. Kauschke, V. Vorliček, and M. Cardona, Solid State Commun. **61**, 487 (1987).
[12]W. Kauschke, V. Vorliček, and M. Cardona, Phys. Rev. B **36**, 9129 (1987).
[13]W. Kauschke and M. Cardona, Phys. Rev. B **35**, 9619 (1987).
[14]J. Menéndez, M. Cardona, and L. K. Vodopyanov, Phys. Rev. B **31**, 3705 (1985).
[15]W. Kauschke, M. Cardona, and E. Bauser, Phys. Rev. B **35**, 8030 (1987).
[16]W. Kauschke, A. K. Sood, M. Cardona, and K. Ploog, Phys. Rev. B **36**, 1612 (1987).
[17]R. M. Martin, Phys. Rev. B **4**, 3676 (1971).
[18]A. A. Gogolin and E. I. Rashba, in *Proceedings of the Thirteenth International Conference on the Physics of Semiconductors,* edited by F. G. Fumi (Tipografia Marves, Rome, 1976), p. 284.
[19]A. K. Ganguly and J. L. Birman, Phys. Rev. **162**, 806 (1967).
[20]R. Zeyher, Chin-Sen Ting, and J. L. Birman, Phys. Rev. B **10**, 1725 (1974).
[21]R. J. Elliott, Phys. Rev. **108**, 1384 (1957).
[22]L. D. Landau and E. M. Lifshitz, *Quantum Mechanics,* Vol. 3 of *Course of Theoretical Physics* (Pergamon, Oxford, 1977), p. 117.
[23]See Ref. 22, p. 662.
[24]A. Cantarero, C. Trallero-Giner, and M. Cardona (unpublished).
[25]D. D. Sell and P. Lawaetz, Phys. Rev. Lett. **26**, 311 (1971).
[26]T. Takizawa, J. Phys. Soc. Jpn. **52**, 1057 (1983).
[27]V. N. Bessolov, T. T. Dedegkaev, A. N. Efimov, N. F. Karlenki, and Yu. F. Ykovlev, Fiz. Tverd. Tela (Leningrad) **22**, 2834 (1980) [Sov. Phys.—Solid State **22**, 1652 (1980)].
[28]See, for example, N. W. Ashcroft and N. D. Mermin, *Solid State Physics,* (Holt, Rinehart and Winston, New York, 1981).
[29]D. E. Aspnes and A. A. Studna, Phys. Rev. B **27**, 985 (1983).
[30]G. A. Samara, Phys. Rev. B **27**, 3494 (1983).
[31]*Landolt-Börnstein Tables,* edited by O. Madelung, H. Schulz, and H. Weiss (Springer, Berlin, 1982), Vol. III/22a.